

**Interface formation between metal and poly-dialkoxy-*p*-phenylene vinylene**F. J. J. Janssen, L. J. van IJzendoorn,\* A. W. Denier van der Gon, M. J. A. de Voigt, and H. H. Brongersma  
*Department of Applied Physics, Eindhoven University of Technology, P.O. Box 513, 5600 MB Eindhoven, The Netherlands*

(Received 18 February 2004; revised manuscript received 14 June 2004; published 29 October 2004)

In this work we address the dynamics and stability of calcium/PPV and barium/PPV interfaces during and after deposition of the metal. Diffusion of calcium and barium into OC<sub>1</sub>C<sub>10</sub> PPV is studied with low energy ion scattering (LEIS) and x-ray photoelectron spectroscopy (XPS). During metal deposition the diffusivity is found to be orders of magnitude higher than after deposition and the diffusion coefficient was found to be dependent on the metal concentration in the PPV. Furthermore, the amount of metal inside the polymer films was found to depend on the deposition rate. These observations were explained in a two-stage diffusion model. In the first stage atoms land on the surface and diffuse fast into the polymer and in the second stage metal ionizes and is trapped and diffusion is strongly decreased. The diffusion coefficient of barium into PPV at  $T=298$  K is found to be almost an order of magnitude lower than the diffusion coefficient of calcium into PPV [ $(0.35\pm 0.05)\times 10^{-23}$  m<sup>2</sup>/s and  $(2.7\pm 0.4)\times 10^{-23}$  m<sup>2</sup>/s, respectively]. Furthermore, the activation energy of the diffusion process of barium into PPV ( $0.75\pm 0.07$  eV) is significantly higher than the activation energy of the diffusion process of calcium into PPV ( $0.62\pm 0.05$  eV). The difference in diffusion coefficient and activation energy between calcium and barium are discussed in terms of an Arrhenius law of diffusion. Finally, polymer LED performance was studied as a function of the amount of metal diffused into the polymer layer. It was observed that the light output and the efficiency decreased as the amount of metal in the PPV increased. This indicates that the metal ions form charge carrier traps and exciton quenching sites in the PPV.

DOI: 10.1103/PhysRevB.70.165425

PACS number(s): 68.35.Fx, 81.05.Lg, 85.60.Jb

**I. INTRODUCTION**

Since the discovery of light emitting conjugated polymers<sup>1</sup> polymer light emitting diodes (PLEDs) have received much attention.<sup>2-4</sup> Polymer based devices are considered promising candidates for full color, cheap and flexible displays. The most simple PLEDs consist of an emitting polymer layer [often derivatives of poly-*p*-phenylene-vinylene (PPV)] sandwiched between an anode [usually ITO (indium tin oxide)] and a cathode (e.g., Ca, Ba, Al).

In previous studies on interface formation between calcium and PPV the focus was mainly on the electronic structure of the interface.<sup>5,6</sup> The dynamics and the stability of the metal/PPV interface have not received much attention so far. However, it was suggested<sup>7</sup> that the interface stability does play an important role in PLED degradation. Diffusion of metals into PPV derivatives and PPV model systems during deposition has been observed,<sup>8-12</sup> but the dynamics of the diffusion process was not investigated. Furthermore, it has been shown that PLEDs with barium cathodes have better efficiencies and longer lifetimes than devices with calcium cathodes.<sup>7</sup> The suggestion was made that metal diffusion and doping could be the reason for this observation. However, for deposition of barium on a PPV derivative with oxygen containing sidegroups it is found that a BaO overlayer is formed,<sup>12</sup> inhibiting diffusion.

In this paper we focus on the diffusion of calcium and barium into OC<sub>1</sub>C<sub>10</sub>-PPV. Diffusion coefficients are derived from time-dependent low energy ion scattering (LEIS) measurements and activation energies of diffusion are derived from temperature dependent measurements. The diffusion coefficients and activation energy are used to describe the diffusion of calcium and barium into PPV with a diffusion model.

For noble metals, it has been observed that slow deposition leads to higher amounts of metal inside the polymer film,<sup>13</sup> therefore we also investigated the influence of the deposition rate on the interface formation.

Finally, the consequences of metal diffusion into PPV films on polymer LED performance (efficiency and light output at a specific voltage) were investigated. Therefore polymer LEDs with cathodes prepared under various conditions were characterized.

**II. EXPERIMENT****A. Low energy ion scattering (LEIS) and x-ray photoelectron spectroscopy (XPS)**

In principle low energy ion scattering<sup>14</sup> (LEIS) characterises the elemental composition of the outermost atomic layer of a sample. A beam of low energy noble gas ions ( $3\text{ keV }^3\text{He}^+$  and  $^4\text{He}^+$  in our case) is directed onto the sample and the energy spectrum of the backscattered ions is measured for one specific scattering geometry (the scattering angle is  $145^\circ$ ). The energy of a backscattered ion depends on the mass of the target atom and, therefore, the energy spectrum of scattered ions reflects the atomic mass distribution of the sample surface. The incoming ions that do not scatter at atoms in the outermost layer, penetrate the sample and are neutralized. LEIS is surface-sensitive because the analyzer of the detection system only accepts ions.<sup>14</sup> Furthermore, the analyser is rotational symmetric and accepts ions over a  $320^\circ$  azimuthal range which greatly enhances the sensitivity and makes it possible to perform measurements with very low doses ( $\sim 3 \times 10^{12}$  ions/cm<sup>2</sup>) and thus low sample damage.<sup>15</sup>

When measuring calcium or barium surfaces with LEIS the interpretation of the experiment becomes more complex

because the reionization probability of these materials is very high.<sup>16</sup> As a consequence, He ions that are neutralized upon penetration of the sample can be reionized upon emerging from it. Thus not only calcium/barium atoms at the surface, but also calcium/barium atoms which are located below the surface contribute significantly to the LEIS spectrum. The He atoms lose energy along their trajectories in the sample and therefore calcium/barium in deeper layers leads to a continuum at the low energy side of the calcium/barium surface peak in the LEIS spectrum.

XPS measurements were performed with Mg  $K\alpha$  radiation ( $E=1253.6$  eV) from a VG twin anode source using the same analyzer as in the LEIS experiments. The samples were tilted  $45^\circ$  with respect to the analyzer. The samples were measured on consecutive times after deposition. Between two measurements the samples were moved away from the x-ray beam to prevent extensive sample damage.

### B. Sample preparation

Glass/ITO/PPV samples used for LEIS/XPS measurements were prepared as follows. The glass/ITO (100 nm ITO, Merck) substrates were first cleaned by ultrasonic treatment and successively with acetone (Uvasol, Merck) and 2-propanol (Uvasol, Merck) each for 10 min. Subsequently 20 min of ozone treatment was performed. After ozone treatment, the preparation chamber was evacuated and flushed with nitrogen. Next, the samples were transferred to a glove box ( $O_2$  and  $H_2O < 1$  ppm) without getting into contact with air and  $OC_{10}C_{10}$  PPV (poly [2-methoxy,5-(2'-ethyl-hexoxy)-p-1,4-phenylene vinylene]) was spin-coated from a 0.5 wt. % PPV in toluene solution onto the glass/ITO substrates. Next, the samples were transported in an airtight container in a nitrogen atmosphere to the LEIS/XPS setup. In a separate compartment of the LEIS/XPS setup calcium or barium was evaporated and in some cases heat treatment was performed. The pressure during evaporation of calcium and barium was  $\sim 1 \times 10^{-7}$  mbar. The deposition process was done for one sample at the time. The LEIS experiments were carried out with 3 keV He<sup>+</sup> ions ( $^3\text{He}^+$  for calcium and  $^4\text{He}^+$  for barium) in a background pressure of  $2 \times 10^{-10}$  mbar and the dose was  $(3 \text{ to } 5) \times 10^{12}$  ions/cm<sup>2</sup> per measurement.

For PLED preparation, substrates of glass covered with ITO were cleaned as described above and an  $OC_{10}C_{10}$ -PPV layer was spin-coated. Then, the specimens were transferred from the glove box into the transfer chamber of the evaporation setup without contact to air. Next, the transfer chamber was pumped down to  $5 \times 10^{-7}$  mbar in about 20 min and the samples were transported to the evaporation chamber. Here a 80 nm thick calcium cathode was evaporated from an effusion cell. The deposition rate was varied between 0.3 nm/s and 0.003 nm/s for both calcium and barium, by varying the evaporation temperature between  $380^\circ\text{C}$  and  $500^\circ\text{C}$  (in this range calcium and barium have almost identical vapour pressure). The pressure during evaporation was  $\sim 1 \times 10^{-7}$  mbar; the residual gas consisted almost entirely of hydrogen (the partial oxygen and water pressures were lower than the detection limit of our mass spectrometer ( $< 10^{-9}$  mbar). Elec-

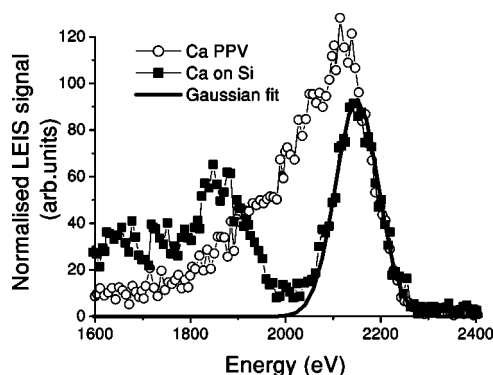


FIG. 1. Typical LEIS spectra of calcium on PPV and of calcium on silicon (Ca surface coverage  $24 \pm 2\%$ ) measured with 3 keV  $^3\text{He}$  ions. The calcium peak in the spectrum of the Ca/Si sample is not broadened and represents the shape of the calcium surface peak. The feature at  $\sim 1850$  eV and the continuum at energies below 1850 eV in the Ca/Si spectrum are originating from helium ions scattered at silicon. The calcium peak in the spectrum obtained from the Ca/Si is fitted with a Gaussian peak. Width and position parameters of this fit were used to derive the calcium surface peak from spectra measured on Ca/PPV samples. This was done by overlaying the high energy side of the calcium peak of the Ca/PPV with the Gaussian peak determined from the Ca on Si. The calcium peak measured on Ca/PPV samples is broadened at the low energy side, because of reionization of  $^3\text{He}$  ions scattered at calcium in deeper layers. Thus to obtain equal surface coverage much more calcium is needed on PPV than on silicon.

trical and optical characteristics were measured in the glove-box and here also impedance spectroscopy was performed.

## III. RESULTS

### A. Diffusion of calcium and barium into PPV

First the interface formation between calcium and  $OC_{10}C_{10}$ -PPV and calcium and silicon will be described. Calcium was deposited onto PPV films and on silicon substrates until the surface was for  $\sim 25\%$  covered with calcium as measured with LEIS; see Fig. 1. On silicon, calcium will form an overlay at the surface while on PPV calcium will diffuse during deposition.<sup>17</sup> Thus to achieve a surface coverage of  $\sim 25\%$  on PPV much more calcium than the equivalent of  $\sim 25\%$  of a monolayer is needed (a total of  $\sim 3 \times 10^{15}$  at/cm<sup>2</sup> calcium was deposited). The peak broadening at the low energy side of the calcium peak measured on Ca/PPV samples (Fig. 1) indicates that no sharp interface is formed.<sup>17</sup> Note that surface roughness of the PPV does not influence the width of the calcium peak in the LEIS spectrum. The maximum of the calcium peak in the LEIS spectrum measured on a PPV film covered for  $24 \pm 2\%$  with calcium is found at slightly lower energy compared to the calcium peak in a LEIS spectrum measured on silicon sample covered with  $24 \pm 2\%$  calcium (Fig. 1). The calcium peak measured on the Ca/PPV sample results from He ions scattered at calcium at the surface and He ions, which penetrate the sample, neutralize, scatter at subsurface calcium and reionize at calcium at the surface. This interpretation of the peak shift was confirmed by measuring a LEIS spectrum

for a thick calcium layer ( $>10$  nm) on silicon. In this case the maximum of the calcium peak was also shifted to lower energies. It is important to note that conversion from the measured yield to a concentration depth profile involves two different conversion factors. The surface contribution can be calculated using the scattering cross section and ion survival probability, while for the subsurface calcium the scattering cross section and the reionisation probability have to be taken into account. Note that the ion survival probability of He ions penetrating in deeper layers is insignificantly small.<sup>14</sup>

From spectra measured on silicon samples with a submonolayer of calcium the position and width of the calcium surface peak can be derived using a Gaussian fit. With the shape parameters of the Gaussian fit, a good estimation of the area of the surface peak in LEIS spectra measured from calcium on PPV can be made.

By measuring LEIS spectra at consecutive times after deposition, it was found that calcium disappears from the surface after deposition. It should be noted that the time scale for the calcium disappearing from the surface is long (a few hours) compared to the evaporation time (120 s). It was verified that calcium really diffuses into the film and does not get oxidized by the residual gas. This was done following the calcium LEIS signal in time of a thick layer of calcium on silicon. In this case the calcium signal did not drop significantly in time. In addition none of the measurements showed an oxygen peak in the LEIS spectrum. Furthermore, XPS measurements did not show a change of the O(1s) peak before and after calcium deposition indicating that no CaO was formed. In order to get a better understanding of the diffusion mechanism a simple Fickian model has been applied to fit the data. As a first approximation a model was adopted in which at  $t=0$  s a planar layer of calcium is present at the surface ( $x=0$ ):<sup>18</sup>

$$c(x,t) = \frac{M_t}{(\pi Dt)^{1/2}} e^{-x^2/4Dt}. \quad (1)$$

Here  $c$  is the concentration,  $M$  the total amount of diffusing substance,  $D$  the diffusion coefficient,  $x$  the depth, and  $t$  the time. From LEIS measurements normally only information about the outermost atomic layer is obtained. However, since calcium and barium have a high reionization probability,<sup>16</sup> depth information can be obtained as well. The amount of calcium below the surface is however difficult to quantify due to unknown reionization probabilities. Consequently, the diffusion of the calcium away from the surface was modeled by fitting the decrease of the calcium surface peak area.

To describe mathematically the decrease of the calcium surface concentration by diffusion we integrate Eq. (1) for  $x=0$  to  $x=x_{LEIS}$ ; this results in

$$M_{LEIS}(t) = \frac{1}{2} M_t \operatorname{erf}(x_{LEIS}/(4Dt)^{1/2}). \quad (2)$$

The area of the surface peak was used to determine the diffusion coefficient and  $x_{LEIS}$  is chosen to be 0.2 nm ( $\sim 1$  monolayer). Note that  $x_{LEIS}$  is directly related to the (square root of the) diffusion constant  $D$ , so by keeping  $x_{LEIS}$  constant, diffusion constants of different measurements can be

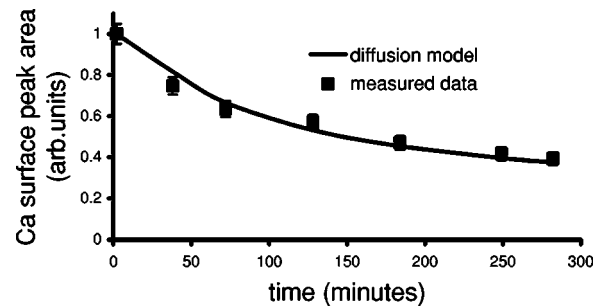


FIG. 2. Calcium surface peak areas measured on a Ca/PPV sample with LEIS as a function of time after deposition. The surface peak area is derived from a Gaussian peak fit to the calcium peak. The diffusion model [Eq. (2)] is fitted through the measured points. A diffusion coefficient of  $D=(2.7\pm 0.4)\times 10^{-23}$  m<sup>2</sup>/s is obtained.

compared, even if  $x_{LEIS}$  is not chosen correctly.  $M_t$  is set to be equal to the normalized LEIS signal at  $t=2$  min (the first data point). The result of the fit of Eq. (2) to the decrease of the calcium surface peak is shown in Fig. 2. A diffusion coefficient for calcium into PPV of  $(2.7\pm 0.4)\times 10^{-23}$  m<sup>2</sup>/s was found. In Sec. IV A the validity of the above-explained approach to describe the diffusion will be discussed.

The diffusion of calcium into PPV was also studied with XPS. By incorporating the concentration profile derived from the diffusion model [Eq. (1)] into the equation for the intensity of the XPS signal,<sup>19</sup> the diffusion coefficient can be derived from the XPS measurements. The diffusion coefficient was derived by fitting the XPS Ca(2p) peak area measured at consecutive times after deposition, with the equation for the intensity of the XPS signal as a function of the concentration profile:

$$I_{XPS} = FS(E)\sigma(E) \int_0^{\infty} c(x)e^{-x/\lambda \cos(\theta)} dx, \quad (3)$$

in which  $F$  is the flux of the incoming x rays,  $S(E)$  is the efficiency of the spectrometer,  $\sigma(E)$  the cross section for photo emission,  $\lambda$  the mean free path of the electron, and  $\theta$  the angle between the surface normal and the direction in which the electrons are emitted ( $45^\circ$  in all our experiments; note that the deviation of this angle caused by the design of the analyzer is one of the main contributions to the error in the diffusion coefficient). In order to simplify the problem, the carbon concentration is considered to be constant in time and the prefactors [ $F$ ,  $S(E)$  and  $\sigma(E)$ ] are collected in a normalization factor; the normalization is done for the first measure point and used for all consecutive points. For the mean free path of electrons ( $\lambda$ ), 3 nm is used, which is an average obtained for polymers.<sup>20</sup> In Fig. 3 the peak area of the Ca(2p) peak is shown as a function of time. The Ca(2p) peak area is normalized to the C(1s) peak area to compensate for fluctuations in the x-ray flux. By doing this, an error is made because the carbon peak area is considered to be constant in time, which is not the case, but this error is much smaller than using the uncorrected data. The intensity of the XPS signal (3) with the concentration profile derived from the

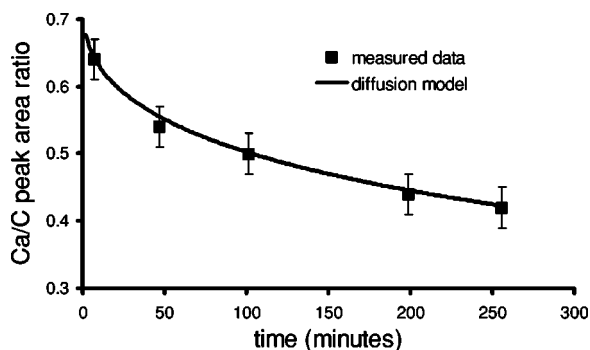


FIG. 3. Calcium ( $2p$ )/carbon ( $1s$ ) XPS peak area ratio measured as a function of time after calcium deposition on to PPV (the initial surface coverage was  $25\pm 2\%$ ). The intensity of the XPS signal (3) with the concentration profile derived from a diffusion model (1) incorporated is fitted through the data points. A diffusion coefficient  $D$  of  $(3\pm 2)\times 10^{-23}$   $\text{m}^2/\text{s}$  is obtained.

diffusion model (1) incorporated is fitted through the data points. From the fit to the XPS measurements (Fig. 3) we obtained a diffusion coefficient for calcium into PPV of  $(3\pm 2)\times 10^{-23}$   $\text{m}^2/\text{s}$  at  $T=298$  K for a surface coverage of calcium of  $25\pm 2\%$ . From LEIS a diffusion coefficient of  $D=(2.7\pm 0.4)\times 10^{-23}$   $\text{m}^2/\text{s}$  was obtained. Thus with XPS and LEIS within experimental error margins the same diffusion coefficients for calcium diffusion into PPV were obtained.

Until now we focused on the diffusion of calcium into PPV films, but it has been shown<sup>7</sup> that barium as cathode material results in higher efficiencies and longer lifetimes for polymer LEDs. Furthermore, it has been reported that small amounts of Ba (equivalent to  $30\text{ \AA}$ ) give the best results for the PLED efficiency and lifetime.<sup>7</sup>

In order to investigate differences between calcium and barium diffusion for the used PPV derivative, barium was deposited on PPV and with LEIS the decrease of the surface peak was measured in time. Subsequently, the diffusion coefficient was derived as described before for calcium diffusion. It was found that barium diffuses into the PPV and the diffusion coefficient of barium is found to be  $(0.35\pm 0.05)\times 10^{-23}$   $\text{m}^2/\text{s}$  at  $T=298$  K for a surface coverage of  $20\pm 2\%$ . Thus, the diffusion coefficient for barium in PPV is about an order of magnitude smaller than the diffusion coefficient for calcium in PPV.

### B. Activation energy of diffusion

Physical insight into diffusion mechanisms is generally obtained by measuring the activation energy of the diffusion process. Therefore, the diffusion coefficients of calcium and barium into PPV were determined at different sample temperatures. These measurements were performed by heating the sample after the measurement of the first LEIS spectrum and thus after the deposition of the metal. This is done to avoid deposition on a heated substrate, which will certainly change the diffusion during deposition and therefore the initial conditions of the experiment.

For a number of temperatures diffusion coefficients were derived as described in Sec. III A. The results for calcium

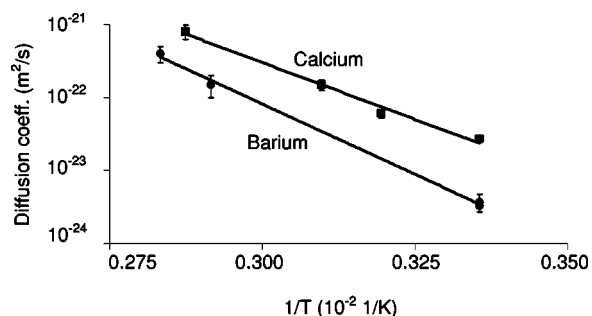


FIG. 4. Temperature dependence of the diffusion coefficient measured with LEIS for both calcium and barium diffusion into PPV for surface coverage of  $25\pm 2\%$  and  $20\pm 2\%$ , respectively. Equation (4) was used to fit the data; we obtained for calcium  $D_0=7\times 10^{-13}$   $\text{m}^2/\text{s}$  and  $E_{act}=0.62\pm 0.05$  eV and for barium  $D_0=3\times 10^{-11}$   $\text{m}^2/\text{s}$  and  $E_{act}=0.75\pm 0.07$  eV.

and barium diffusion into PPV are shown in Fig. 4 for a temperature range from  $25$  to  $80^\circ\text{C}$ . Generally, an Arrhenius law can describe the temperature dependence of the diffusion coefficients:<sup>13</sup>

$$D = D_0 \exp\left(-\frac{E_{act}}{kT}\right), \quad (4)$$

in which  $D$  is the diffusion coefficient,  $D_0$  the preexponential factor, and  $E_{act}$  the activation energy.  $E_{act}$  is usually interpreted as the energy barrier the ion has to overcome to jump to the next potential minimum. The interpretation of the preexponential factor  $D_0$  depends on the diffusion model, but  $D_0$  is generally considered proportional to the vibrational frequency of the diffusing species in the potential minimum, which is determined by the local environment.  $D_0$  and  $E_{act}$  will be discussed in more detail for calcium and barium diffusion into PPV in Sec. IV C.

Calcium and barium diffusion into PPV are clearly found to be activated processes. From Fig. 4 an activation energy of  $0.62\pm 0.05$  eV is obtained for calcium into PPV and  $D_0$  was determined to be  $7\times 10^{-13}$   $\text{m}^2/\text{s}$ . For barium diffusion into PPV an activation energy of  $0.75\pm 0.07$  eV was found and  $D_0$  was determined to be  $3\times 10^{-11}$   $\text{m}^2/\text{s}$ . The accuracy of the pre-exponential factor is typically within one order of magnitude.

### C. Comparison between high and low metal deposition rates

It is well known from literature that the diffusion of (non-reactive) metals into polymers can depend on the metal deposition rate.<sup>13</sup> To find out whether the diffusion of Ca and Ba into PPV also depends on the deposition rate a series of experiments was performed with different evaporation temperatures, thereby varying the flux of metal atoms onto the polymer surface. It should be noted that the difference in thermal energy between the “slow” and “fast” deposited atoms ( $T_{slow}\sim 380^\circ\text{C}$  and  $T_{fast}\sim 500^\circ\text{C}$ ) is small ( $\delta kT$  is  $\sim 0.01$  eV) compared to the activation energy for diffusion as found in the previous paragraph.

Figure 5 shows LEIS spectra of calcium and barium deposited “fast” ( $\sim 3\times 10^{13}$   $\text{at}/\text{cm}^2\text{s}$ ) and “slow” ( $\sim 4$

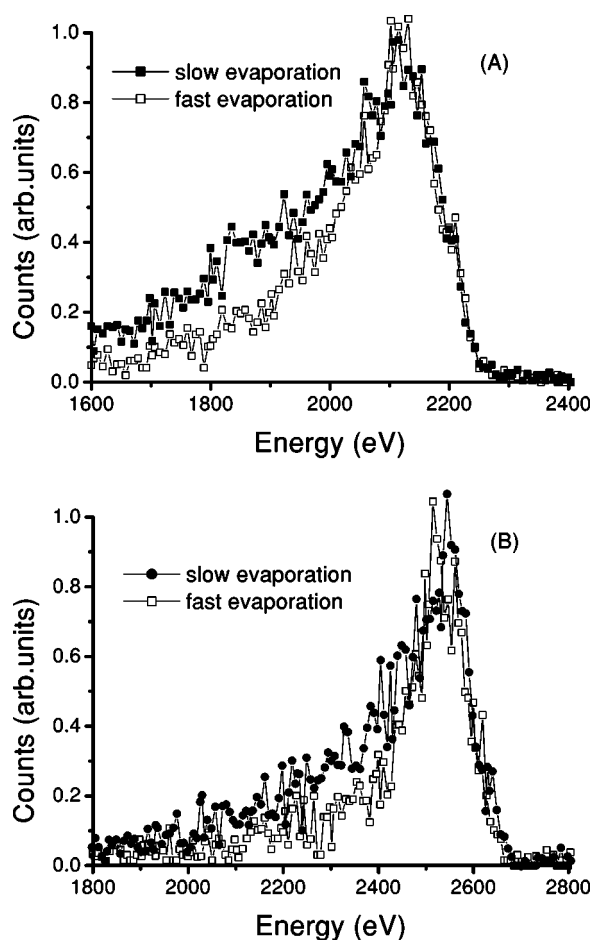


FIG. 5. Normalized LEIS spectra of calcium (a) and barium (b) on PPV measured with 3 keV  $^3\text{He}^+$  and  $^4\text{He}^+$ , respectively. The metal surface coverage was  $24 \pm 2\%$  for calcium and  $20 \pm 2\%$  for barium. In the “fast” deposition experiments the metal was deposited in  $\sim 60$  s ( $\sim 3 \times 10^{13}$  at/cm $^2$  s) while in the “slow” deposition experiments it was deposited in  $\sim 15$  min ( $\sim 4 \times 10^{12}$  at/cm $^2$  s). The He ion dose was kept very low ( $\sim 3 \times 10^{12}$  at/cm $^2$ ) in order to prevent extensive sample damage.

$\times 10^{12}$  at/cm $^2$ s) onto PPV. It is clear that right after deposition (2 min) a lower amount of subsurface metal is present for “fast” deposited samples than for “slowly” deposited samples.

The first spectrum measured on the “slowly” deposited sample was compared to a series of LEIS spectra measured on the “fast” deposited sample. This was done to determine whether the large amount of subsurface metal present in “slowly” deposited samples directly after deposited, was

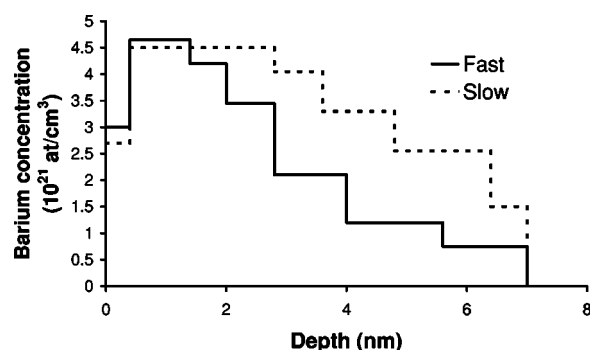


FIG. 6. Depth profiles of barium in PPV for slow and fast deposition [Fig. 5(b)] as calculated from fits to the LEIS data with an adapted version of TRIM (Ref. 22). A precise description of the simulation procedures can be found in Ref. 23.

caused by the long time ( $\sim 15$  min) between the moment the first metal atom impeded on the sample and the first measurement. In none of the “fast” deposited spectra the amount of signal at lower energies was found to be comparable to the amount of signal in the “slowly” deposited spectrum. This implies that *during* deposition much more calcium penetrates the sample than *after* deposition. Note also that if the evaporation time was increased for the “fast” deposition case, both the amount on the surface as well as the amount in deeper layers increases (see Sec. III D). Thus the difference between “slow” and “fast” deposition is a real physical one and not just a difference in timing of the processes.

If the reionization probability for He on PPV is assumed to be zero and the fraction of He atoms that are reionized by calcium is assumed to be linear with the surface calcium coverage, calcium depth profiles can be calculated from a LEIS spectrum. First the complete LEIS spectrum is scaled, making the calcium surface peak equal to the surface peak in a LEIS spectrum of a sample with a thick calcium layer ( $>10$  nm). Subsequently, the concentration is obtained by dividing the signal of reionized He ions by the signal of the reionized He ions of a thick layer of calcium. The depth scale is derived using the stopping power presented in Ref. 21. The results for the spectra of Ca on PPV presented in Fig. 5 are shown in Table I.

For barium on PPV simulations of the LEIS experiments are performed using a modified version of the ion beam simulation program TRIM.<sup>22</sup> A precise description of the simulations is given by de Ridder *et al.*<sup>23</sup> The obtained barium depth distribution for the LEIS spectra presented in Fig. 5 is shown in Fig. 6. Clearly, the amount of metal below the surface is larger for low deposition rates.

TABLE I. Amount of calcium at specific depths in the PPV layer, as a function of deposition rate. The concentrations are retrieved from the LEIS spectra presented in Fig. 5(a); for the depth scales, stopping powers from Ref. 21 were used.

| Depth | Concentration at 2 nm ( $\times 10^{21}$ at/cm $^3$ ) | Concentration at 4 nm ( $\times 10^{21}$ at/cm $^3$ ) | Concentration at 6 nm ( $\times 10^{21}$ at/cm $^3$ ) |
|-------|---|---|---|
| Fast  | $7.6 \pm 0.5$   | 4.2   | 2.2   |
| Slow  | 7.7   | 6.0   | 3.3   |

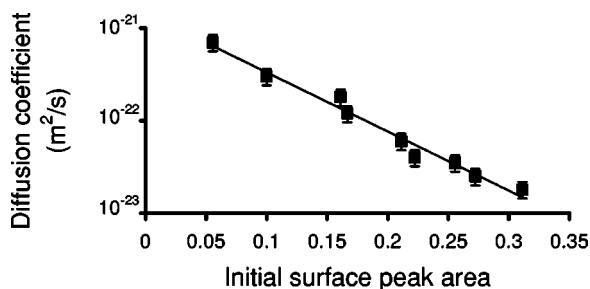


FIG. 7. Diffusion coefficients of calcium into PPV as a function of the initial surface coverage at  $T=298$  K as obtained from LEIS measurements. The deposition speed was kept constant for all the coverages. The full line is an exponential fit through the data points.

Note that the metal concentrations in the outermost layer of the polymer are smaller than the metal concentrations directly below the surface. Diffusion of metal into the polymer is enhanced because of the high surface energy of metals compared with polymers, making it energetically favorable for metal atoms to be situated below the sample surface. This will be discussed in more detail in Sec. IV B. For both fast and slow deposition, more calcium than barium is present below the surface pointing to a higher calcium diffusion coefficient during deposition.

The results presented in this paragraph establish that interface formation depends on the flux of metal atoms to the surface during deposition.

#### D. Dependence of the diffusion coefficient on the metal concentration

In the previous paragraph we concluded that the metal diffusion in PPV depends on the flux of metal atoms coming to the surface. In this paragraph the flux of calcium atoms coming ( $\sim 3 \times 10^{13}$  at/cm<sup>2</sup>s) to the surface was kept constant but the evaporation time was varied.

Figure 7 shows the dependence of the diffusion coefficient derived with Eq. (2), on the amount of calcium deposited (concentration at the surface). Figure 7 indicates that the metal diffusion coefficient is concentration dependent. The measured data was fitted with an exponential equation implicitly assuming that the diffusion coefficient changes linearly with the surface concentration:

$$\frac{\partial D}{\partial c_s} = -ac_s. \quad (5)$$

Here  $c_s$  is the initial surface concentration and  $a$  is a constant;  $a$  is found to be  $14.7 \pm 0.5$ . By extrapolation of the fit to zero surface coverage the diffusion coefficient of a single ion is estimated to be  $150 \times 10^{-23}$  m<sup>2</sup>/s.

To get an indication of the diffusion coefficient during deposition, we fitted the depth profile, measured directly after deposition, with Eq. (1). The depth profile shown in Fig. 8 was made by subtraction of the fitted surface peak from the LEIS spectra and by conversion of the energy scale with the stopping powers presented in Ref. 21. This profile is formed within 3 min, which results in a diffusion coefficient of  $(3000 \pm 500) \times 10^{-23}$  m<sup>2</sup>/s.

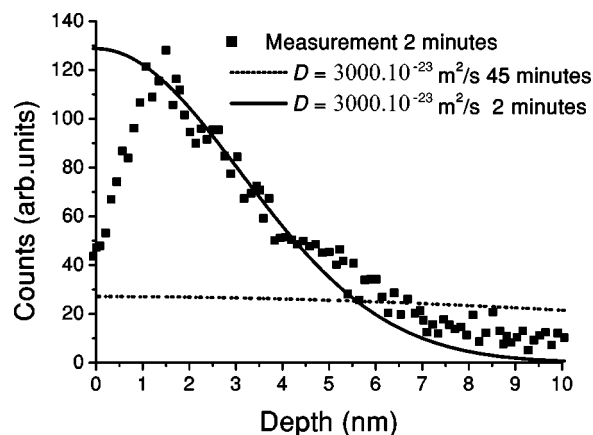


FIG. 8. Depth profile of the calcium 2 min after deposition; the profile is obtained from the LEIS measurement. The depth scale is calculated with the stopping powers measured in Ref. 21. The contribution of the He ions scattered from the surface was subtracted. A diffusivity of  $(3000 \pm 500) \times 10^{-23}$  m<sup>2</sup>/s was found appropriate to fit the data. To indicate that the diffusion after deposition is slowed down dramatically the calculated depth profile after 45 min with  $D=3000 \times 10^{-23}$  m<sup>2</sup>/s is also shown; the curve measured after 45 min (not shown for clarity reasons) is only slightly different from the spectrum after 2 min.

Note that by applying Eq. (1) a constant diffusion coefficient is assumed, while even during the early stages of deposition the diffusion coefficient is expected to continuously decrease when the metal concentration increases. Consequently the application of Eq. (1) leads to an underestimation of the initial diffusion coefficient. Apparently the calcium diffusion speed during deposition is even larger than the estimate based on Fig. 8 and also much larger than the single ion diffusion coefficient after deposition derived from Fig. 7. Apparently, the diffusion process during deposition differs from the diffusion process after deposition (see Sec. IV B).

In order to find out more about the diffusion process during deposition, we derived the amount of calcium at specific depths for different surface coverage. The flux of metal atoms to the surface was again kept constant; the result is shown in Table II. From Table II it can be seen that during the early stages of deposition the diffusion coefficient is high and metal can diffuse fast to large depths. In the later stages calcium also can diffuse to a deeper layer but on average more calcium is confined near the surface, indicating that the average diffusion coefficient decreases.

#### E. PLED performance

In the previous paragraphs we addressed the diffusion of calcium and barium into PPV. When polymer LEDs with calcium and barium cathodes are compared it is difficult to interpret their behavior in terms of diffusion, because apart from differences in metal diffusion coefficients, the work functions of the metals are different which alters the electron injection into the PPV and the device efficiency. We found on comparing devices with calcium and barium cathodes somewhat better performance for devices with barium cathodes (more light output and higher efficiencies for compa-

TABLE II. Calcium concentration at specific depths in the PPV layer, as a function of surface coverage. The concentrations are retrieved from the LEIS spectra; for conversion from energy to depth scales, stopping powers presented in Ref. 21 were used.

| Depth                | Concentration at<br>2 nm ( $\times 10^{21}$ at/cm <sup>3</sup> ) | Concentration at<br>4 nm ( $\times 10^{21}$ at/cm <sup>3</sup> ) | Concentration at<br>6 nm ( $\times 10^{21}$ at/cm <sup>3</sup> ) |
|----------------------|--|--|--|
| 16 $\pm$ 2% coverage | 6.3 $\pm$ 0.5  | 3.6  | 2.0  |
| 24 $\pm$ 2% coverage | 7.6  | 4.2  | 2.2  |

erable currents) as seen by CaO *et al.*<sup>7</sup> However, it can certainly not be concluded that diffusion is the only important parameter for this observation.

However a comparison is possible between devices with the same cathode material deposited on different deposition rates. PLEDs were produced with a calcium cathode of  $\sim 80$  nm. The deposition rate for “fast” deposited devices was 0.3 nm/s. For the “slowly” deposited devices the deposition rate of the first 20 nm was 0.003 nm/s; the remaining 60 nm was deposited at 0.3 nm/s. In Fig. 9 current-voltage and light output-voltage curves of these devices are shown. The PLEDs were electro-optically characterized in vacuum ( $\sim 10^{-9}$  mbar) one hour after calcium deposition to exclude thermal effects. Figure 9 shows that devices with “fast” deposited cathodes have the highest light output at 6 volts. Devices with “slowly” deposited cathodes have a light output that is about 50% lower at 6 volts and have an efficiency which is 15% lower. The time needed to deposit the cathode is obviously different for the two deposition rates which could lead to different sample temperatures during deposition as a result of radiative heating by the evaporator. This might also influence the device characteristics.<sup>17</sup> However, in our experiments the temperatures measured on the glass of the PLED immediately after deposition are equal (38°C) for both deposition speeds. In the case of slow deposition, the calcium at the PPV interface is exposed longer to impurities (e.g., oxygen), which might be present in the vacuum. The decrease in current cannot be explained by oxidation during deposition since it is not accompanied by a strong decrease in efficiency, which was observed in experiments where oxygen was deliberately added during deposition.<sup>24</sup> In addition,

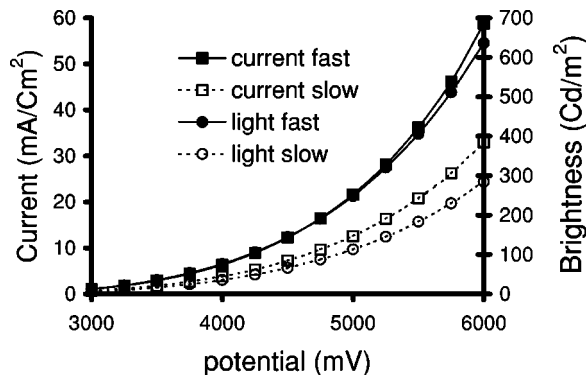


FIG. 9. Comparison between current-voltage and brightness-voltage characteristics for PLEDs with calcium cathodes deposited “fast” (0.3 nm/s) and “slow” (0.003 nm/s). The lines connecting the points are drawn to guide the eye.

our mass spectrometer did not detect impurities in the vacuum, which means that the partial pressures of oxygen and water vapor were below  $10^{-9}$  mbar.

For barium similar behavior as for calcium was observed, but the difference between “slow” and “fast” deposition was considerable smaller. The current and light output dropped with only 20% at 6 volts and the efficiency with 15%.

It can be concluded that “slow” deposition, which leads to more metal in the polymer films near the interface with the cathode (Fig. 5), results in decreased PLED light output. As already suggested by Park *et al.*<sup>25</sup> the metal in the polymer near the interface may trap electrons and/or lead to nonradiative exciton decay. To verify explicitly the influence of the metal on trapping of electrons, impedance spectroscopy measurements were performed. It was shown<sup>26</sup> that hole and electron mobilities can be derived from the difference in the complex admittance measured at zero bias and at a bias at which the devices operates. Figure 10 shows the negative differential susceptance  $[-\Delta B = -\omega(C - C_0)]$ , which is derived from the frequency dependent capacitance at 0 V ( $C_0$ ) and at 2.75 V ( $C$ ). The electron signal is strongly influenced for “slowly” deposited devices while the hole signal stays more or less equal, indicating that the electron trapping and/or injection is altered.

In addition the effect of “fast” and “slowly” deposited cathodes on the electroluminescence spectra were investigated for glass/ITO/PPV/calcium devices. Figure 11 shows that the amount of calcium diffused into the layer does influence the process leading to electroluminescence. Apparently “slow” deposition selectively suppresses the (0-0) vibronic transition.

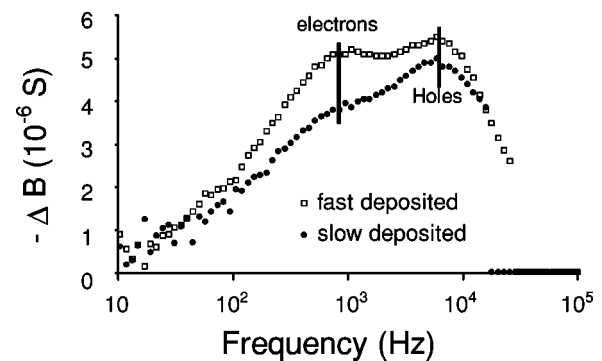


FIG. 10. Impedance spectroscopy measurements on devices with calcium cathodes deposited “fast” (0.3 nm/s) and “slow” (0.003 nm/s). The differential susceptibility  $[-\Delta B = -\omega(C_{2.75} - C_0)]$  is plotted as a function of the frequency. The frequency dependence of the capacitance was measured at 0 V and at 2.75 V. The electron and the hole peak are indicated (Ref. 26).

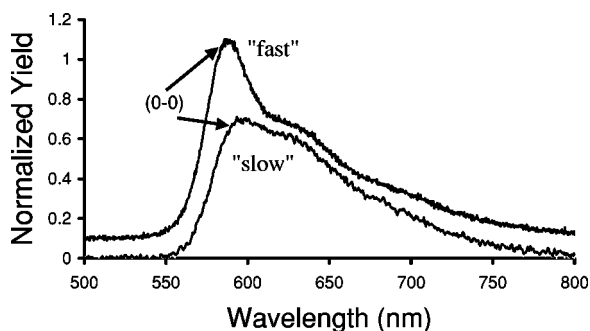


FIG. 11. Electroluminescence spectra of glass/ITO/PPV/Ca device with “fast” and “slow” deposited cathodes. The position of the (0-0) vibronic transition is indicated. For clarity, the spectra of the “fast” deposited curve has an offset of 0.1.

It was shown by Hu *et al.*<sup>27</sup> that deposition of different cathode materials resulted in changes in the electroluminescence spectra. These authors suggested that the first vibronic transition (0-0) is dominated by interface effects. This is in agreement with our observations. The calcium that diffused into the PPV apparently quenches the excitons close to the Ca/PPV interface where most of the calcium is present. This is also indicated by the decrease of the device efficiency.

## IV. DISCUSSION

### A. Validation of the diffusion model

Before the diffusion of calcium and barium into PPV is compared and discussed, first the validity of the diffusion model will be discussed. In Sec. III A we fitted the decrease of the surface peak with a diffusion model with a concentration independent diffusion coefficient and we assumed all the metal to be on top of the PPV a  $t=0$  s. With LEIS the diffusion coefficient of calcium into PPV was found to be  $(2.7 \pm 0.4) \times 10^{-23} \text{ m}^2/\text{s}$ . However, in Secs. III C and III D it was found that the diffusion coefficient strongly depends on the metal concentration. Besides, during deposition the diffusion coefficient is high and relatively large quantities of metal diffuse into the polymer layer.

Consequently a model is required that describes the concentration dependent diffusion and further takes into account the metal flux during deposition. Unfortunately no analytical model is available to describe this behavior.<sup>18</sup> More important, depth profiles during deposition are required to obtain the dependence of the diffusion coefficient on the concentration during deposition. However, after deposition the concentration profile near the surface does not change over orders of magnitude on the time scales at which our measurements are performed. Therefore we assume that the diffusion coefficients we obtained are representative for the diffusion coefficients of calcium and barium ions in a metal/PPV environment, close to the cathode/polymer interface in a PLED.

In order to check whether the diffusion coefficient varies significantly over the depth range studied, we estimated the diffusion coefficient near the front end of the calcium in the PPV. A relatively high diffusion coefficient is expected at the low concentrations near the end of the profile. We estimated

the diffusion coefficient near the end of the profile by the shift of the depth at which the calcium concentration equals  $\sim 10\%$ . When the shift is assumed to be proportional to  $(D\Delta t)^{1/2}$ , the diffusion coefficient was found to be  $(10 \pm 3) \times 10^{-23} \text{ m}^2/\text{s}$ , which is only 3 times higher than the diffusion coefficient obtained from the decrease of the surface peak.

It is also possible to derive the calcium diffusion coefficient from the change in the measured depth profile after the deposition (similar as demonstrated in Fig. 8). The diffusion coefficient obtained for the change of the depth profile between  $t=2$  min and  $t=267$  min is found to be  $(7 \pm 3) \times 10^{-23} \text{ m}^2/\text{s}$ .

The three methods to estimate the diffusion coefficient of calcium into PPV indicate that the diffusion coefficient varies less than a factor of 3 over the entire depth profile after metal deposition. The high surface energy leading to lower concentration of metal at the surface compared to metal in deeper layers (Fig. 6), apparently does not influence the diffusion after deposition significantly.

It can be concluded that in spite of the fact that the concentration dependent diffusion coefficient is not incorporated in the mathematical model, it nevertheless can be used to provide insight in the diffusion of calcium and barium into PPV.

## B. Interface formation

### 1. Introduction

In Secs. III C and III D the diffusion coefficient of calcium into PPV was shown to depend on the metal concentration. Furthermore, it was found that diffusion is particularly fast during the early phases of deposition; after deposition an orders of magnitude lower diffusion coefficient is found. Additionally, the metal diffusion depends on the deposition rate (see Fig. 5); lower deposition rates lead to more metal in the polymer film. Here, we try to envisage a model describing all these observations.

### 2. Clustering

Clustering of metal atoms may be the origin of the difference in metal depth distribution resulting from differences in deposition rate.<sup>13</sup> The physical origin of clustering is minimization of the contact area of metal atoms with the polymer or vacuum (reducing the surface energy); the metal-polymer interaction must be relatively low for clustering to occur. The formation of clusters has been found for nonreactive materials (Au and Ag) in TMC-PC (polycarbonate bisphenoltrimethyl cyclohexane) layers and was found to depend on the deposition rate; for fast deposition clusters are only found at the surface (finally a metallic overlayer is formed), for slow deposition cluster formation also appeared subsurface.<sup>13</sup>

For nonreactive materials (Au, Ag) cluster formation was also found on PTCDA.<sup>28</sup> For reactive materials (Al, Ti, Sn and In) metal diffuses into the PTCDA in the early stages of deposition, while in later stage a closed overlayer is formed. The number of reactive atoms deposited before a closed overlayer is formed was found to depend strongly on the material and it ranged from  $2 \text{ \AA}$  ( $7.4 \times 10^{14} \text{ at}/\text{cm}^2$ ) for tin to



100 Å ( $3.8 \times 10^{16}$  at/cm<sup>2</sup>) for indium. Calcium and barium are reactive metals, consequently cluster formation is not likely to occur during the early stages of deposition on PPV as considered in our experiments.<sup>28</sup> Furthermore, ions do not tend to cluster due to Coulomb repulsion.<sup>28</sup>

To investigate whether cluster formation plays a role in our experiments, transmission electron microscopy (TEM) was performed. Glass/ITO/PPV substrates with calcium or barium surface coverages of  $3 \pm 1\%$  up to  $30 \pm 2\%$  were prepared. Subsequently, the PPV film was released from the ITO and TEM measurements through the complete film were performed (the PPV thickness was  $\sim 30$  nm in this case). No evidence of clustering was obtained. The resolution of the TEM images was  $\sim 5$  nm. Thus these measurements provide us with an upper limit for the size of clusters of approximately 5 nm ( $\sim 1000$  atoms).

### 3. Cross-linking of polymer chains by metal ions

The temperature dependence of the diffusion coefficient of Au and Ag in BPA-PC (biphenol A polycarbonaat) has been shown by Faupel *et al.*<sup>13</sup> and no discontinuity was found at the glass transition temperature of the polymer. This behavior was explained in terms of physical cross-linking of the polymer chain by the metal. Silvian *et al.*<sup>29</sup> suggested physical cross-linking of polyethyleneterephthalate (PET) by Al, Ag and Cu atoms to explain the increased of cohesion of the polymer film. More reactive materials (Fe and Ni) are even reported to catalyze cross-linking of polyethylene and poly(tetrafluoroethylene) (PTFE) systems.<sup>30</sup>

Physical cross-linking will immobilize the polymer/metal system; decrease the mobility of the polymer chains, and consequently lower the diffusion of the metal by increasing the activation energy for conformational changes. The amount of metal in the polymer film is expected to determine the degree of cross-linking and therefore an exponential relation can be expected between the diffusion coefficient and the metal concentration. We found that the metal concentration determines the diffusion coefficient and consequently metal ion induced physical cross-linking is able to explain the concentration dependence in our experiments. However the observed deposition rate dependence of the metal depth profile is difficult to explain in terms of physical cross-linking.

### 4. A qualitative description of the diffusion process

Apparently, both the formation of small clusters and metal induced cross-linking of polymer chains seem to be required to explain all experimental observations. The experimental findings are consistent with a qualitative model description that assumes two consecutive processes to occur for metal atoms that land on the surface.

(1) Fast migration/diffusion of the neutral atom, which can occur both at the surface, or into the polymer matrix.

(2) Ionization of the reactive metal atom which traps the metal at a specific site in the polymer matrix.

The initial fast migration process can be responsible for the measured concentration profile immediately after deposition. Note that the high surface energy of the metals com-

pared to the polymers favors metal diffusion into the bulk. During this stage neutral atoms can also cluster which explains the dependence of the metal depth profile on the deposition rate. Shortly after this initial phase (estimate duration  $\sim$  seconds) the reactive calcium and barium atoms will interact with the polymer matrix, ionize and become trapped. The trapping of metal ions can be associated with the physical cross-linking of the polymer chains as described in Sec. IV B 3. Note that the trapping is not irreversible, but leads to a higher activation energy for diffusion and a higher preexponential ( $D_0$ ) due to the reduced mobility of the polymer chains in the physical cross-linked polymer network. As a result, an increasing number of calcium atoms that land on the surface will be ionized at or near the surface (see Table II) and experience both a diffusion barrier by the ionized calcium trapped in the polymer as well as the reduced chain mobility in the cross-linked polymer matrix. This process apparently reduces the formation of large clusters near the surface for submonolayer coverage and explains the relatively slow diffusion process on the time scales measured in our LEIS experiments.

The decrease of the surface concentration, which is used to determine the diffusion coefficient, can be considered to be the diffusion coefficient of metal ions into the polymer layer. The diffusion coefficient is mainly determined by the trap depth, the Coulomb repulsion and the cross-linking. The higher calcium diffusion coefficient deep in the PPV layers (see Sec. III D) results from the fact that the Coulomb repulsion and cross linking is lower in deep layers.

### C. Comparison between calcium and barium diffusion

Our experiments clearly show that the diffusion coefficient and activation energies for diffusion of calcium and barium ions into PPV differ considerably. At room temperature the diffusion coefficients differ an order of magnitude and the activation energy of barium is higher than the activation energy of calcium (Fig. 4).

In this paragraph we will discuss possible causes for the differences between calcium and barium diffusion in terms of activated diffusion [Eq. (4)]. First the difference in the activation energy ( $E_{act}$ ) between calcium and barium will be discussed and subsequently the differences in the preexponential factor ( $D_0$ ).

We measured activation energies of diffusion for  $0.62 \pm 0.05$  eV for calcium into PPV and  $0.76 \pm 0.07$  for barium into PPV. The activation energy for diffusion has two contributions, a component representative for the energy required to accommodate the diffusing species by polymer deformation (straining the polymer matrix) and a component representative for the binding at a site in the polymer matrix.<sup>31-33</sup> The first term is related to the size of the diffusing species; larger species require a higher energy to migrate. The influence of the physical size of the diffusing species on the diffusion coefficient has been shown for gases in polymers, which are characterised by little or no interaction between gas and the polymer.<sup>34</sup> In this case, the activation energy was found to be correlated with diameter;<sup>35</sup>  $E_{act} \sim d^2$ . To get an indication of the effect of size difference on the acti-

vation energy for calcium and barium diffusion, we can estimate the difference in activation energy between non-interacting species with the sizes of calcium and barium ions and PPV. Unfortunately activation energy data of a noninteracting species in a PPV is not available in literature. In glassy polymer however typically an activation energy of  $\sim 0.3$  eV is found for oxygen.<sup>13,36,37</sup> Using  $E_{act} \sim d^2$  and an activation energy of 0.3 eV for oxygen molecules the activation energy of a non-interacting species with the size of a barium ion can be estimated to be  $\sim 0.1$  eV higher than the activation energy of a non-interacting species with the size of a calcium ion. Note that for the non-spherical oxygen molecule a corrected diameter was used.<sup>13</sup>

Obviously, for metal diffusion in polymers, the interaction between the polymer and the metal is also important. From XPS measurements it has been shown that interaction between PPV and calcium occurs.<sup>5,6,8,38</sup> The influence of interaction on the diffusion can be determined by comparing diffusion coefficients from interacting and noninteracting species in PPV, which are comparable in size. The diffusion coefficient of (noninteracting) oxygen in OC<sub>1</sub>C<sub>10</sub> PPV is many orders of magnitude higher ( $D=10^{-9}$  m<sup>2</sup>/s at  $T=298$  K)<sup>39</sup> than the diffusion coefficient for calcium and barium into PPV that we measured. The diffusion coefficient of calcium is lower than the diffusion coefficient for oxygen in spite of the fact that the contribution to the activation energy of the conformational rearrangement should be lower for calcium ( $d_{Ox}^2 > d_{Ca}^2$ ). These observations indicate that the chemical interaction is an important factor. In contrast to the large difference between the binding energy of calcium and oxygen with PPV, the difference in binding energy between calcium and PPV and barium and PPV is expected to be small, but probably not insignificant and therefore can also explain (part) of the difference in activation energy between calcium and barium.

The diffusion coefficient of calcium and barium in PPV is not only determined by the activation energy but also by the preexponential factor  $D_0$  [see Eq. (4)]. For calcium we obtained  $D_0=7 \times 10^{-13}$  m<sup>2</sup>/s and for barium  $D_0=3 \times 10^{-11}$  m<sup>2</sup>/s was found. The preexponential factor  $D_0$  can be expressed as<sup>13</sup>

$$D_0 = \alpha a^2 v e^{S/k}, \quad (6)$$

in which  $a$  is the average jump distance of the ion,  $\alpha$  a factor depending on structure of the polymer and the correlation between successive jumps,  $v$  is the vibration frequency,  $S$  the entropy of diffusion and  $k$  the Boltzman constant;  $D_0$  can be considered as a fingerprint for the environment.<sup>13</sup> If  $D_0$  behaves according to this model it will vary for elements with different mass when the structure related parameters  $\alpha$  and  $S$  are independent on the diffusing species, because the vibration frequency ( $v$ ) is mass dependent (it varies as  $m^{-1/2}$ ).<sup>13,31</sup> The factor  $D_0 m^{1/2}$  should then be similar for calcium and barium diffusion into PPV. However, in our case we find for barium  $D_0 m^{1/2} = 4 \times 10^{-10}$  m<sup>2</sup>(amu)<sup>1/2</sup>/s and for calcium  $D_0 m^{1/2} = 4 \times 10^{-12}$  m<sup>2</sup>(amu)<sup>1/2</sup>/s. Apparently the entropy ( $S$ ) is the factor that dominates the value of  $D_0$ . The contribution

of the entropy ( $S$ ) in Eq. (6) is determined by the number of possible states available to a diffusing metal ion and is linked to the mobility of the polymer chains in the (physical cross linked) matrix. Thus the diameter of the diffusing ion will influence the entropy. Our observation is that  $D_{0,Ba} \gg D_{0,Ca}$  is consistent with observations of Krevelen and Hoftyzer<sup>36</sup> who showed that for noninteracting species,  $D_0$  increases exponentially with increasing activation energy.

Concluding, the individual metal ions are most likely trapped in potential minima. Transport occurs by hopping from site to site and both interaction between the metal and conformational changes of the polymer matrix contribute to the activation energy.

The difference of  $D_0$  between calcium and barium diffusion into PPV is most likely correlated with differences in perturbation of the local environment for calcium and barium (because  $d_{Ca} < d_{Ba}$ ), which is associated with a difference in entropy of diffusion.

#### D. Device performance

In Sec. III E it has been shown that devices fabricated with high metal concentration in the PPV layer near the cathode (“slow” deposition) have lower light output at specific voltages and a slightly lower efficiency compared to devices with low metal concentration in the PPV film (“fast” deposition). Obviously, an increased concentration of metal near the interface leads to more gap states and quenching sites for excitons.<sup>25</sup> Lower injection and/or more trapping of electrons was observed from  $I$ - $V$  characterization and impedance measurements.

Electroluminescence spectra show that not only the electron injection decreases when more metal ions are present in the film, but also the electrically excited states of PPV shift which alters the electroluminescence spectrum.

#### V. CONCLUSIONS

During deposition the diffusivity is found to be orders of magnitude higher than after deposition and the diffusion coefficient was found to be dependent on the metal concentration in the PPV. Furthermore, the amount of metal inside the polymer films was found to depend on the deposition rate. These observations were explained in a two-stage diffusion model. In the first stage atoms land on the surface and diffuse fast into the polymer and in the second stage metal ionizes and is trapped and diffusion is strongly decreased. In this model clustering (in the first stage) can explain the dependence of the amount of metal in the polymer on the deposition rate. Metal induced physical cross-linking and ion repulsion can explain the dependence of the diffusion coefficient on the metal concentration.

The diffusion coefficient at room temperature of barium into PPV is almost an order of magnitude lower than the diffusion coefficient of calcium into PPV. This was explained in terms of the activation energy of diffusion ( $E_{act}$ ) and the preexponential factor  $D_0$ , which was obtained from temperature dependent measurements of the diffusion coefficient with LEIS. The activation energy of barium is found to be

higher than the activation energy of calcium, the smaller size of the calcium ion and the difference in polymer-metal interaction are the most likely causes for these observations. The  $D_0$  of barium is found to be higher than the  $D_0$  of calcium which is most likely correlated with a different perturbation of the local environment by calcium and barium, caused by the size difference between calcium and barium ions.

PLED performance is strongly related to cathode formation. It was found that reducing the deposition speed, which results in an increase of the amount of calcium inside the PPV, leads to lower electron injection and/or more electron

trapping and consequently lower efficiency and light output of the polymer LEDs.

#### ACKNOWLEDGMENTS

We would like to thank Dr. X. Yang of Eindhoven University of Technology for performing Transmission Electron Microscopy measurements, Dr. ir. M. de Ridder of Calipso BV for performing TRIM simulations, and Dr. H. F. M. Schoo of the TNO Institute of Industrial Technology for useful discussion. The research of F.J.J.J. is part of the DPI programme.

\*Author to whom correspondence should be addressed at Cyclotron 2.13, Department of Applied Physics, Eindhoven University of Technology, Post-Box 513, 5600 MB Eindhoven, The Netherlands. FAX: +31-40-2438060, Email address: L.J.van.IJzendoorn@tue.nl

- <sup>1</sup>J. H. Burroughes, D. D. C. Bradley, A. R. Brown, R. N. Marks, K. Mackey, R. H. Friend, P. L. Burn, and A. B. Holmes, *Nature (London)* **347**, 539 (1990).
- <sup>2</sup>D. Braun and A. J. Heeger, *Appl. Phys. Lett.* **58**, 1982 (1991).
- <sup>3</sup>C. D. Muller, A. Falcou, N. Reckefuss, M. Rojahn, V. Wiederhirn, P. Rudati, H. Frohne, O. Nuyken, H. Becker, and M. Meerholz, *Nature (London)* **421**, 829 (2003).
- <sup>4</sup>R. H. Friend, R. W. Gymer, A. B. Holmes, J. H. Burroughes, R. N. Marks, C. Taliani, D. D. C. Bradley, D. A. Dos Santos, J. L. Brédas, M. Lögdlund, and W. R. Salaneck, *Nature (London)* **397**, 121 (1999).
- <sup>5</sup>W. R. Salaneck and M. Lögdlund, *Polym. Adv. Technol.* **9**, 419 (1998).
- <sup>6</sup>E. Eteddgui, H. Razafitrimo, K. T. Park, Y. Gao, and B. R. Hsieh, *Surf. Interface Anal.* **23**, 89 (1995).
- <sup>7</sup>Y. Cao, G. Yu, I. D. Parker, and A. J. Heeger, *J. Appl. Phys.* **88**, 3618 (2000).
- <sup>8</sup>P. Dannelun, M. Fahlman, C. Fayquet, K. Kaerjama, Y. Sonada, R. Lazzaroni, J. L. Brédas, and W. R. Salaneck, *Synth. Met.* **67**, 133 (1994).
- <sup>9</sup>P. Dannelun, M. Lögdlund, C. Fredriksson, R. Lazzaroni, C. Fauquet, S. Stafström, C. W. Spangler, J. L. Brédas, and W. R. Salaneck, *J. Chem. Phys.* **100**, 6765 (1994).
- <sup>10</sup>G. G. Andersson, H. H. P. Gommans, A. W. Denier van der Gon, and H. H. Brongersma, *J. Appl. Phys.* **93**, 3299 (2003).
- <sup>11</sup>J. Birgerson, M. Fahlman, P. Broems, and W. R. Salaneck, *Synth. Met.* **80**, 125 (1996).
- <sup>12</sup>A. Crispin, A. Jonsson, M. Fahlman, and W. R. Salaneck, *J. Chem. Phys.* **115**, 5252 (2001).
- <sup>13</sup>F. Faupel, R. Willecke, and A. Thran, *Mater. Sci. Eng., R.* **22**, 1 (1998).
- <sup>14</sup>H. H. Brongersma and H. J. van Daal, in *Analysis of Microelectronic Materials and Devices*, edited by M. Grasserbauer (Wiley, New York, 1991), Chap. 2.8.
- <sup>15</sup>K. J. Hook, J. A. Gardella, Jr., and L. Sakvati, Jr., *Macromolecules* **20**, 2112 (1987).
- <sup>16</sup>R. Souda, T. Aizawa, C. Oshima, and Y. Ishizawa, *Nucl. Instrum. Methods Phys. Res. B* **45**, 364 (1990).
- <sup>17</sup>F. J. J. Janssen, Ph.D. thesis, Eindhoven University of Technology, 2004; F. J. J. Janssen, J. M. Sturm, A. W. Denier van der Gon, L. J. van IJzendoorn, M. Kemerink, H. F. M. Schoo, M. J. A. de Voigt, and H. H. Brongersma, *Org. Electron.* **4**, 209 (2003).
- <sup>18</sup>J. Crank, *The Mathematics of Diffusion*, 2nd ed. (Oxford University Press, New York, 1975).
- <sup>19</sup>J. W. Niemantsverdriet, *Spectroscopy in Catalysis: An Introduction* (VCH Verlag, Weinheim, 1993).
- <sup>20</sup>P. J. Cumpston, *Surf. Interface Anal.* **31**, 23 (2001).
- <sup>21</sup>G. Andersson and H. Morgner, *Nucl. Instrum. Methods Phys. Res. B* **155**, 357 (1999).
- <sup>22</sup>J. P. Biersack, E. Steinbauer, and P. Bauer, *Nucl. Instrum. Methods Phys. Res. B* **61**, 77 (1991).
- <sup>23</sup>M. de Ridder, F. J. J. Janssen, E. Steinbauer, L. J. IJzendoorn, and H. H. Brongersma (unpublished).
- <sup>24</sup>G. G. Andersson, M. P. de Jong, F. J. J. Janssen, J. M. Sturm, L. J. van IJzendoorn, A. W. Denier van der Gon, M. J. A. de Voigt, and H. H. Brongersma, *J. Appl. Phys.* **90**, 1376 (2001).
- <sup>25</sup>Y. Park, V. E. Choong, B. R. Hsieh, C. W. Tang, and Y. Gao, *Phys. Rev. Lett.* **78**, 3955 (1997).
- <sup>26</sup>H. C. F. Martens, P. W. M. Blom, and H. F. M. Schoo, *Phys. Rev. B* **61**, 7489 (2000).
- <sup>27</sup>B. Hu and F. E. Karasz, *Chem. Phys.* **227**, 263 (1998).
- <sup>28</sup>Y. Hirose, A. Kahn, V. Aristov, P. Soukiassian, V. Bulovic, and S. R. Forrest, *Phys. Rev. B* **54**, 13 748 (1996).
- <sup>29</sup>J. F. Silvian, A. Veyrat, and J. J. Ehrhardt, *Thin Solid Films* **221**, 114 (1992).
- <sup>30</sup>S. L. Vogel and H. Schonhorn, *J. Appl. Polym. Sci.* **23**, 495 (1979).
- <sup>31</sup>J. Philibert, *Atom Movements Diffusion and Mass Transport in Solids* (Les Editions Physique, Les Ulis Cedex, France, 1991).
- <sup>32</sup>H. R. Glyde, *Rev. Mod. Phys.* **39**, 373 (1967).
- <sup>33</sup>C. Wert and C. Zener, *Phys. Rev.* **76**, 1169 (1949).
- <sup>34</sup>L. M. Costello and W. J. Koros, *J. Polym. Sci., Part B: Polym. Phys.* **32**, 701 (1994).
- <sup>35</sup>J. Crank and G. S. Park, *Diffusion in Polymers* (Academic, London and New York, 1968).
- <sup>36</sup>D. W. Krevelen and P. J. Hoftyzer, *Properties of Polymers* (Elsevier, Amsterdam, 1976).
- <sup>37</sup>J. Brandrup and E. H. Immergut, *Handbook of Polymers* (Wiley, New York, 1989).
- <sup>38</sup>F. J. J. Janssen, Ph.D. thesis, Eindhoven University of Technology, 2004; F. J. J. Janssen, A. W. Denier van der Gon, R. Tholen, L. J. van IJzendoorn, M. J. A. de Voigt, and H. H. Brongersma (unpublished).
- <sup>39</sup>B. H. Cumpston, I. D. Parker, and K. F. Jensen, *J. Appl. Phys.* **81**, 3716 (1997).